



# Lawrence Berkeley Laboratory

UNIVERSITY OF CALIFORNIA

## Materials & Molecular Research Division

Submitted to Physical Review B

CLUSTER-VARIATION METHOD FOR THE TRIANGULAR  
LATTICE GAS I. THREE-SUBLATTICE POINT APPROXIMATION

R. Osório and L.M. Falicov

August 1980

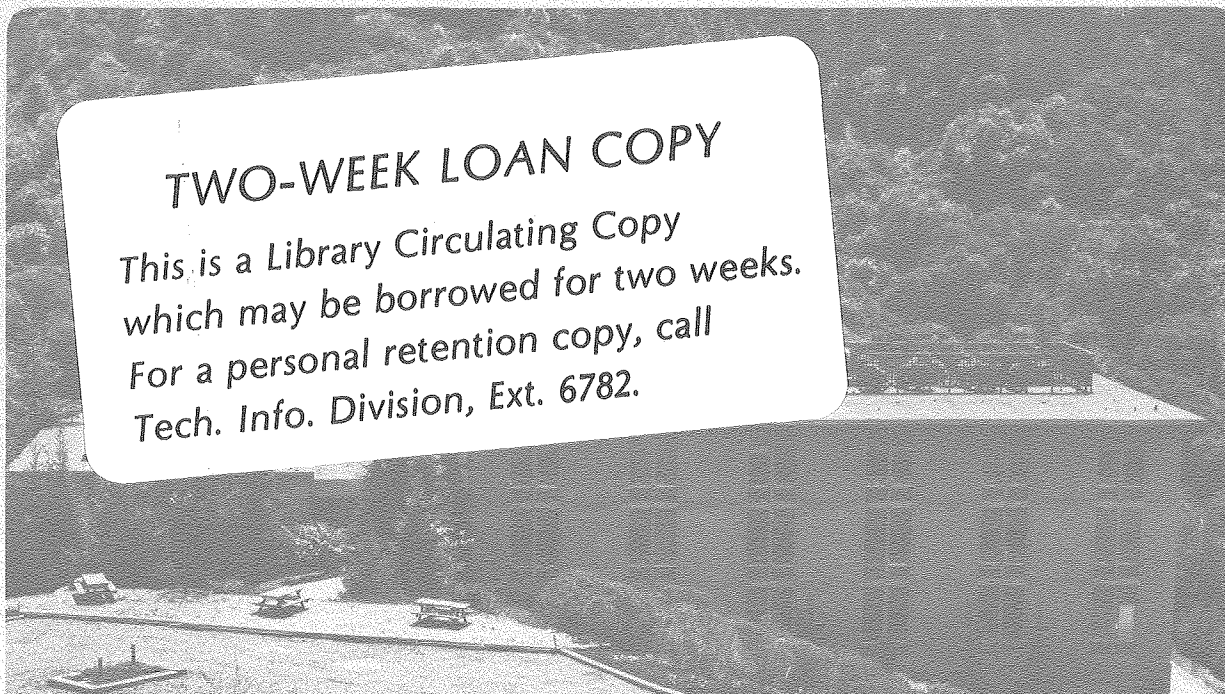
RECEIVED  
LAWRENCE  
BERKELEY LABORATORY

NOV 6 1980

LIBRARY AND  
DOCUMENTS SECTION

### TWO-WEEK LOAN COPY

This is a Library Circulating Copy  
which may be borrowed for two weeks.  
For a personal retention copy, call  
Tech. Info. Division, Ext. 6782.



LBL-11474 c. 2

## **DISCLAIMER**

This document was prepared as an account of work sponsored by the United States Government. While this document is believed to contain correct information, neither the United States Government nor any agency thereof, nor the Regents of the University of California, nor any of their employees, makes any warranty, express or implied, or assumes any legal responsibility for the accuracy, completeness, or usefulness of any information, apparatus, product, or process disclosed, or represents that its use would not infringe privately owned rights. Reference herein to any specific commercial product, process, or service by its trade name, trademark, manufacturer, or otherwise, does not necessarily constitute or imply its endorsement, recommendation, or favoring by the United States Government or any agency thereof, or the Regents of the University of California. The views and opinions of authors expressed herein do not necessarily state or reflect those of the United States Government or any agency thereof or the Regents of the University of California.

Cluster-variation method for the triangular lattice gas  
I. Three-sublattice point approximation

R. Osório and L.M. Falicov

Materials and Molecular Research Division, Lawrence  
Berkeley Laboratory and Department of Physics, University  
of California, Berkeley, California 94720

The triangular lattice gas is examined as a model for the ordering of  $\text{Li}^+$  ions in intercalated transition metal dichalcogenides. A three-sublattice Bragg-Williams (point approximation) calculation illustrates the meaning of the features in the incremental capacity versus concentration curves: (a) minima are associated with ordered structures, (b) sharp maxima (divergences) are caused by the coexistence of ordered and disordered phases over small concentration intervals and (c) smooth maxima can be found at concentrations of no direct relevance to ordering.

## 1. INTRODUCTION

A triangular lattice gas model for the problem of ordering of  $\text{Li}^+$  ions in the system  $\text{Li}_x\text{TiS}_2$  was recently proposed by Thompson<sup>1</sup> and studied by Berlinsky et al.<sup>2</sup> through a renormalization group calculation. In this and the following<sup>3</sup> paper (hereafter referred to as II) we use Kikuchi's<sup>4</sup> cluster-variation method to explore the problem further, including a discussion of the effects of three-body potentials on thermodynamic functions and on the order-disorder phase diagram.

Lithium has been intercalated into the layered transition-metal dichalcogenides<sup>5</sup> (represented by  $\text{MX}_2$ , where M is a transition metal and X a chalcogen) to form compounds of the type  $\text{Li}_x\text{MX}_2$  ( $0 \leq x \leq 1$ ), that have found use as cathodes in batteries. The system  $\text{Li}_x\text{TiS}_2$  has been particularly successful<sup>6</sup> due to its reversibility and rapid lithium self-diffusion.

In  $\text{Li}_x\text{TiS}_2$ ,  $\text{Li}^+$  ions reside between two  $\text{TiS}_2$  layers, at sites which make themselves a two-dimensional triangular network (these are the octahedral sites found between the two-dimensional triangular layers of sulphur, each S layer belonging to a different S-Ti-S sandwich). The practical uses of this material have prompted a large number of experiments<sup>5-9</sup> including chemical, electrochemical and nuclear magnetic resonance studies.

Thompson<sup>1</sup> has performed accurate measurements of the voltage  $V$  versus concentration  $x$  relationship in the electrochemical cell where  $\text{Li}_x\text{TiS}_2$  is produced. The data showed well defined peaks in the incremental capacity ( $-\partial x/\partial V$ ) at constant temperature, the main peaks appearing at  $x=1/9$ ,

1/4 and 6/7. Thompson suggested that these peaks are associated with the formation of two-dimensional ordered superlattices of the  $\text{Li}^+$  ions at those concentrations.

The experiments were performed in a Li-electrolyte- $\text{Li}_x\text{TiS}_2$  cell and the measured voltage gives the difference between the chemical potentials of the  $\text{Li}^+$  ion in the  $\text{Li}_x\text{TiS}_2$  cathode and the Li anode. If the Li anode is considered a  $\text{Li}^+$  reservoir, the voltage  $V$  is given by

$$|e|V = \text{constant} - \mu_1 \quad (1.1)$$

where  $\mu_1$  is the  $\text{Li}^+$  chemical potential in  $\text{Li}_x\text{TiS}_2$ . The value of  $\mu_1$  is determined by a variety of factors: lattice distortions, lattice vibrations, electron screening, etc. The main effect however is caused by the  $\text{Li}^+$ - $\text{Li}^+$  Coulomb repulsion and by the resultant collective effects. The nearest-neighbor interaction is the dominant part of the energy, since the repulsion between two ions is screened by the electrons in neighboring  $\text{TiS}_2$  layers.

In this paper we study the phase diagram of a lattice gas of particles interacting through a nearest-neighbor repulsion in a triangular arrangement. The problem has been previously investigated by the Bethe-Peierls method<sup>10</sup>, a simplified triangle cluster approximation<sup>11</sup>, renormalization group techniques<sup>2,12</sup> and a Monte-Carlo calculation<sup>13</sup>.

In this paper we show that a model as simple as a generalized Bragg-Williams<sup>14</sup> approximation (equivalent to Kikuchi's model with points as the basic clusters) for three sublattices gives the correct physical picture for experimental features in the  $(-\partial x/\partial V)$ -versus- $x$  curves for systems

like  $\text{Li}_x\text{TiS}_2$ . A better approximation is used in II. Our calculation is presented in Section 2 and the Appendix. A discussion of the results is the subject of Section 3.

## 2. CALCULATION

As illustrated in Figure 1, the triangular lattice is divided into three interpenetrating sublattices,  $\alpha$ ,  $\beta$ , and  $\gamma$ , such that any site in one of them, say  $\alpha$ , has three nearest neighbors in each of the other two sublattices,  $\beta$  and  $\gamma$ . This representation can be justified by the work of Kanamori and Kaburagi<sup>15,16</sup>, who found the ground-state structures for the triangular lattice gas with various pairwise interactions. In our notation, for nearest-neighbor repulsions only, we have the following equilibrium configurations: for  $x=1/3$  the  $\alpha$  sublattice full,  $n_\alpha=1$ , with empty  $\beta$  and  $\gamma$  sublattices,  $n_\beta=n_\gamma=0$ ; for  $x=2/3$  the  $\alpha$  and  $\beta$  sublattices full,  $n_\alpha=n_\beta=1$ , and the  $\gamma$  sublattice empty,  $n_\gamma=0$ . We define by  $n_\nu$  ( $\nu=\alpha,\beta,\gamma$ ) the probability that a lattice site of sublattice  $\nu$  is occupied by an ion. We thus have

$$x = \frac{1}{3}(n_\alpha + n_\beta + n_\gamma) \quad (2.1)$$

If there are  $N$  sites in the lattice, the interaction energy is approximated by

$$E = NU [n_\alpha n_\beta + n_\beta n_\gamma + n_\gamma n_\alpha] \quad (2.2)$$

where  $U$  is the nearest-neighbor interaction energy ( $U>0$ ). The entropy is taken to be the sum of the Bragg-Williams entropies for the three sublattices:

$$S = k_B \sum_v \ln \frac{(N/3)!}{(Nn_v/3)! [N(1-n_v)/3]!} \quad (2.3)$$

In both Equations (2.2) and (2.3) short-range correlations between the sites are ignored.

The temperature  $T$  and the free energy  $F=E-TS$  are hereafter expressed in the dimensionless forms

$$\tau = \frac{k_B T}{U}, \quad f = \frac{F}{NU} \quad (2.4)$$

The use of Stirling's approximation in Eq. (2.3) yields for the reduced free energy the result

$$f = n_\alpha n_\beta + n_\beta n_\gamma + n_\gamma n_\alpha + \frac{\tau}{3} \sum_v [n_v \ln n_v + (1-n_v) \ln (1-n_v)] \quad (2.5)$$

Because of the constraint in Eq. (2.1) only two of the three sublattice probabilities  $n_v$ , say  $n_\alpha$  and  $n_\beta$ , should be considered as independent variables for a given concentration  $\underline{x}$ . The equilibrium configuration of the lattice gas (i.e., the values of  $n_\alpha$ ,  $n_\beta$  and  $n_\gamma$ ) can be found for given values of  $\underline{x}$  and  $\tau$  by minimizing  $\underline{f}$  in Eq. (2.5) with respect to  $n_\alpha$  and  $n_\beta$ . The reduced chemical potential

$$\mu = \frac{\mu_1}{U} \quad (2.6)$$

is then given as the derivative  $(\partial f / \partial x)$ .

An alternative method is to consider  $\mu$  as the thermodynamic parameter instead of  $\underline{x}$ . Now the three sublattice proba-

bilities are independent variational parameters for the minimization of the grand potential

$$\Omega = F - \mu_1 N x \quad .$$

The concentration  $x$  is obtained from Eq. (2.1) after  $\Omega$  has been minimized.

Although both methods are mathematically equivalent, they are for convenience applied to different regions of the  $(x, \tau)$  plane to obtain a phase diagram. The procedure is described in the Appendix and the phase diagram is shown in Figure 2. The complete phase diagram displays a mirror symmetry around the line  $x = \frac{1}{2}$ . This is a consequence of the pairwise, concentration-independent nature of the assumed interactions, leading to a particle-hole symmetry, which is translated by the relations

$$n_\alpha(x=x_0) = 1 - n_\gamma(x=1-x_0) \quad (2.7a)$$

and

$$n_\beta(x=x_0) = 1 - n_\beta(x=1-x_0) \quad . \quad (2.7b)$$

It can then be readily shown that

$$f(x=x_0) = f(x=1-x_0) + 6x_0^{-3} \quad , \quad (2.8)$$

$$\mu(x=x_0) = 6 - \mu(x=1-x_0) \quad (2.9)$$

and

$$\left( \frac{\partial x}{\partial \mu} \right)_{x=x_0} = \left( \frac{\partial x}{\partial \mu} \right)_{x=1-x_0} \quad . \quad (2.10)$$

These relations are not actually satisfied for the system  $\text{Li}_x\text{TiS}_2$  but they seem to be a good approximation for the sequence  $\sqrt[18]{\text{Li}_x \text{Ta}_y \text{Ti}_{1-y} \text{S}_2}$ , with  $0.3 \leq y \leq 0.5$ . In  $\text{Li}_x\text{TiS}_2$ , the interaction between two  $\text{Li}^+$  ions must depend on the concentration, due to the increasing donation of electrons to the  $\text{TiS}_2$  conduction band.

### 3. RESULTS AND DISCUSSION

The different regions in the complete phase diagram are: the disordered phase (3), where  $n_\alpha = n_\beta = n_\gamma$ ; two ordered phases (12) and (21), where one of the sublattice probabilities is different from the other two; and the ordered phase (111), where the three probabilities are different.

A physical insight into the meaning of the different phases may be gained by considering the behavior of the lattice gas at  $T=0$ . The reduced free energy is then given by the broken line in Figure 3. If we increase the concentration of occupied sites, only the  $\alpha$  sublattice is being filled in the interval  $0 < x < 1/3$ , where  $n_\alpha = 3x$ ,  $n_\beta = n_\gamma = 0$ . The  $\beta$  sublattice is filled in the interval  $1/3 < x < 2/3$ , where  $n_\alpha = 1$ ,  $n_\beta = 3x - 1$ ,  $n_\gamma = 0$ . Finally the  $\gamma$  sublattice is filled in the interval  $2/3 < x < 1$ , where  $n_\alpha = n_\beta = 1$ ,  $n_\gamma = 3x - 2$ . Thus at  $T=0$ , for  $1/3 < x < 2/3$  the system is in the (111) phase; otherwise it is in the (12) or the (21) phase. As the temperature increases, the entropy term in the free energy reduces the range of existence of the (111) phase and induces the appearance of a completely disordered phase (3), which emerges from the  $x=0$  and  $x=1$  extremes

of the allowed range of concentrations and occupies the whole concentration range when the reduced temperature exceeds the critical value  $\tau_c = 3/4$ .

The zero-temperature picture discussed above is only valid in the present mean-field approximation, where an ordered phase is required to avoid nearest-neighbor pairs. In II, however, we show that short-range correlations can actually lead to long-range disorder even at  $T=0$ .

The phases (3) and (12) are connected by a first-order phase transition; the phases (12)' and (111) are connected by a second-order phase transition. For a given  $\tau < \tau_c$  there is a small interval of values of  $x$  in each half of the phase diagram where the phases (3) and (12) coexist in a heterogeneous mixture. In this region  $f$  is a linear function of  $x$ , defined by the common tangent to the  $f$ -versus- $x$  curves for the phases (3) and (12), and both the chemical potential and the grand potential are constant. The incremental capacity  $(-\partial x/\partial V)$  is given in our dimensionless units by  $(\partial x/\partial \mu)$ . At  $\tau=0$  this function is zero at  $x=0, 1/3, 2/3, 1$ , and infinite otherwise. It is more convenient to use the function  $(\tau \cdot \partial x/\partial \mu)$  which has slope  $\pm 1$  at  $x=0, 1$  for any value of  $\tau$ . This function is plotted in Figure 4 for several temperatures. For  $\tau > \tau_c$  we have the ordinary one-sublattice Bragg-Williams result

$$\tau \frac{\partial x}{\partial \mu} = \left[ \frac{6}{\tau} + \frac{1}{x(1-x)} \right]^{-1}, \quad (3.1)$$

i.e. a smooth, structureless curve.

Our incremental capacity diverges over the small intervals of  $x$  where the phases (3) and (12) coexist. On the other

hand, no singularities occur at values of the concentration where ordered arrangements of the particles are expected. On the contrary, at small values of  $\tau$ , there are minima of  $(\partial x / \partial \mu)$  near  $x=1/3$  and  $2/3$ , where ordered configurations exist. This is intuitively expected: a significant change in the chemical potential should be required to modify the structure at those concentrations. We thus confirm the conclusions of Berlinsky et al.  $\sqrt{2}$  concerning the meaning of minima and maxima of the incremental capacity. In our model, however, this function diverges over small  $x$ -intervals, rather than only at isolated points.

#### 4. CONCLUSIONS

In this paper we have studied the order-disorder phase diagram for a three-sublattice representation of a triangular lattice gas with a nearest-neighbor repulsive interaction. A "point" approximation was used as the first step towards a more sophisticated triangle cluster approximation, discussed in II. In spite of its simplicity the approximation used here has been able to account qualitatively for the experimental features in the incremental capacity of systems like  $\text{Li}_x\text{TiS}_2$ .

We have found that minima of the incremental capacity occur at the concentrations where ordered structures form and divergences are associated with the coexistence of two phases (one ordered and the other one disordered) and do not necessarily occur at concentrations that can be expressed as rational numbers of small denominator. Smooth maxima (e.g.

at  $x = 1/2$  at any temperature and at  $x \approx 1/6$  and  $x \approx 5/6$  at very low temperatures in our model) can appear at concentrations that are not structurally meaningful and are not related to ordering effects.

#### ACKNOWLEDGMENTS

This work was supported in part by the Division of Material Sciences, U.S. Department of Energy under Contract # W-7405-Eng-48 and by a grant from the Miller Institute for Basic Research in Science in the form of a Miller Professorship (to L.M.F.). One of us (R.O.) would like to thank CNPq and UFPE (Brazil) for financial support.

## APPENDIX

The computation of the phase diagram and the thermodynamic functions was performed in two stages. First, two of the sublattice probabilities were required to be equal. This case includes the phases (3) and (12). The free energy was then minimized at constants  $\underline{x}$  and  $\tau$  with respect to the only one independent sublattice parameter. In the second stage, the (111) phase was calculated by minimizing the grand potential at constant  $\mu$  and  $\tau$  with respect to the three sublattice parameters, now independent.

In the first case, we have the reduced free energy of Eq. (2.5) with

$$n_{\beta} = n_{\gamma} = \frac{1}{2}(3x - n_{\alpha}) \quad . \quad (A.1)$$

At the equilibrium configuration, we have

$$\frac{\partial f}{\partial n_{\alpha}} = \frac{3}{2}(x - n_{\alpha}) + \frac{\tau}{3} \ln \frac{n_{\alpha}(2 - 3x + n_{\alpha})}{(1 - n_{\alpha})(3x - n_{\alpha})} = 0 \quad (A.2)$$

with the restrictions

$$1 \geq n_{\alpha}, n_{\beta} \geq 0 \quad . \quad (A.3)$$

For  $\tau > \tau_c = \frac{3}{4}$ , the disordered phase, defined by  $n_{\alpha} = x$ , is the solution. In general, Eq. (A.2) can be solved by a Newton-Raphson <sup>19</sup> iteration scheme.

When the equilibrium configuration corresponds to the disordered phase, we must have

$$\frac{\partial^2 f}{\partial n_\alpha^2} (n_\alpha = x) = -\frac{3}{2} + \frac{\tau}{2} \frac{1}{x(1-x)} > 0, \quad (\text{A.4})$$

which is true for  $\tau < \tau_c$  only if  $x < x_-$  or  $x > x_+$ , where

$$x_\pm = \frac{1}{2} \pm \left(\frac{1}{4} - \frac{\tau}{3}\right)^{\frac{1}{2}} \quad (\text{A.5})$$

We need only to consider the region  $0 < x < \frac{1}{2}$  because of the particle-hole symmetry discussed in Section 2. For  $x < x_-$ , Eq. (A.4) shows that the function  $f(n_\alpha)$  has a local minimum at  $n_\alpha = x$ . It turns out that this is a global minimum only if  $x < x_0$ , where  $x_0$  is within 0.02 smaller than  $x_-$ . Inside the small interval  $x_0 < x < x_-$ , the global minimum is not at  $n_\alpha = x$  but at the only other minimum at  $n_\alpha > x$ , i.e. in the (12) phase.

When  $x_- < x < \frac{1}{2}$  the function  $f(n_\alpha)$  has a local maximum at  $n_\alpha = x$  and two minima, one at  $n_\alpha < x$  and the other at  $n_\alpha > x$ . From physical reasoning, the solution at  $n_\alpha > x$  must correspond to the equilibrium configuration, since the  $\alpha$  sublattice is the one being filled first at  $T=0$ . The Newton-Raphson procedure converges when the initial point for  $n_\alpha$  is taken to be close to 1 or  $3x$ , whichever is smaller.

For each  $\tau$ , the interval of coexistence of the phases (3) and (12) is determined by plotting the reduced grand potential

$$\omega = \frac{\Omega}{NU} = f - \mu x \quad (\text{A.6})$$

as a function of  $\mu$ . The (3) and (12) curves cross at a certain value of  $\mu$  corresponding to two values of  $x$  ( $= -\partial\omega/\partial\mu$ ), one for

each phase, that define the interval of coexistence. This method is equivalent to drawing the common tangent between the  $\underline{f}$ -versus- $\underline{x}$  curves for the two phases, but our procedure is computationally easier and more accurate.

Finally, for the (111) phase, it is more convenient to start with the reduced grand potential

$$\omega = \frac{9}{2} x^2 + \sum_v y(n_v) , \quad (A.7)$$

where

$$\begin{aligned} y(n_v) = & -\frac{1}{2} (n_v)^2 + \frac{\tau}{3} [n_v \ln n_v \\ & + (1-n_v) \ln (1-n_v)] - \frac{1}{3} \mu n_v . \end{aligned} \quad (A.8)$$

For a given  $\mu$ , at the equilibrium state we must have

$$\frac{\partial \omega}{\partial n_v} = 3x + y'(n_v) = 0 \quad (A.9)$$

where

$$y'(n_v) = -n_v + \frac{\tau}{3} \ln \frac{n_v}{1-n_v} - \frac{\mu}{3} . \quad (A.10)$$

Equations (A.9) and (A.10) can be solved by assigning values to

$$\lambda = -3x + \frac{\mu}{3}$$

and solving the equation

$$g(n_v) \equiv -n_v + \frac{\tau}{3} \ln \frac{n_v}{1-n_v} = \lambda \quad (\text{A.11})$$

by a Newton-Raphson procedure. For  $\tau < \tau_c$ , this equation has three different roots between 0 and 1 whenever  $\lambda$  is such that  $g(x_+) < \lambda < g(x_-)$ , where  $x_+$  and  $x_-$  are defined in Eq. (A.5). In the (111) phase, each sublattice probability must assume the value of a different root. The (111) phase happens to have lower free energy than the other phases at the same concentration.

REFERENCES

1. A.H. Thompson, Phys. Rev. Letters 40, 1511 (1978);  
J. Electrochem. Soc. 126, 608 (1979).
2. A.J. Berlinsky, W.G. Unruh, W.R. McKinnon and R.R. Haering,  
Solid State Commun. 31, 135 (1979).
3. R. Osório and L.M. Falicov, Phys. Rev. B (following paper).
4. R. Kikuchi, Phys. Rev. 81, 988 (1951).
5. D.W. Murphy and R.A. Trumbore, J. Crystal Growth 39,  
185 (1977).
6. M.S. Whittingham, Science 192, 1126 (1976).
7. M.S. Whittingham, J. Electrochem. Soc. 123, 315 (1976).
8. B.G. Silbernagel and M.S. Whittingham, J. Chem. Phys. 64,  
3670 (1976).
9. B.G. Silbernagel, Mat. Sci. and Eng. 31, 281 (1977).
10. C.E. Campbell and M. Schick, Phys. Rev. A 5, 1919 (1972).
11. D.M. Burley, Proc. Phys. Soc. (London), 85, 1163 (1965).
12. M. Schick, J.S. Walker and M. Wortis, Phys. Rev. B 16,  
2205 (1977).
13. B.D. Metcalf, Phys. Letters 45 A, 1 (1973).
14. W.L. Bragg and E.J. Williams, Proc. Roy. Soc. (London)  
A145, 699 (1934). See also C. Barrett and T.B. Massalski,  
Structure of Metals (3rd ed, McGraw-Hill, New York, 1966),  
pp. 284 ff.
15. M. Kaburagi and J. Kanamori, Japan J. Appl. Phys. Suppl.  
2, Pt. 2 (Proc. 2nd Intl. Conf. on Solid Surfaces, Kyoto),  
145 (1974).

16. M. Kaburagi and J. Kanamori, J. Phys. Soc. Japan, 44, 718 (1978).
17. W. Shockley, J. Chem. Phys. 6, 130 (1938).
18. A.H. Thompson, Physica 99B, 100 (1980).
19. See for instance G. Dahlquist and Å. Björck, Numerical Methods (N. Anderson, transl. Prentice-Hall, Englewood cliffs, N.J., 1974), pp. 222 ff.

FIGURE CAPTIONS

Figure 1 Representation of the triangular lattice with its three interpenetrating sublattices.

Figure 2 Phase diagram for the triangular lattice gas in the  $(x, \tau)$  plane. The dashed line is the locus of equal free energies for the (3) and (12) phases.

Figure 3 Reduced energy  $\underline{f}$  as a function of concentration  $\underline{x}$  for  $\tau = 0$ .

Figure 4 Reduced incremental capacity multiplied by reduced temperature  $(\tau \cdot \partial x / \partial \mu)$  as a function of concentration  $\underline{x}$  for (a)  $\tau \rightarrow 0$ , (b)  $\tau = 0.25$ , (c)  $\tau = 0.5$ , (d)  $\tau = 0.7$ .

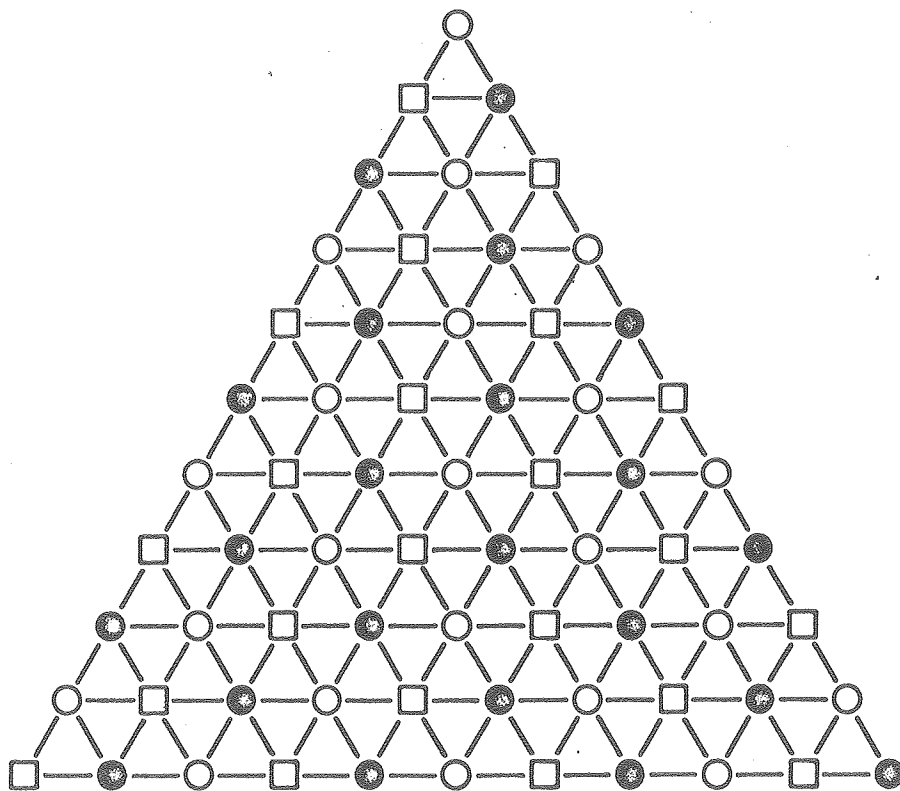


Figure 1

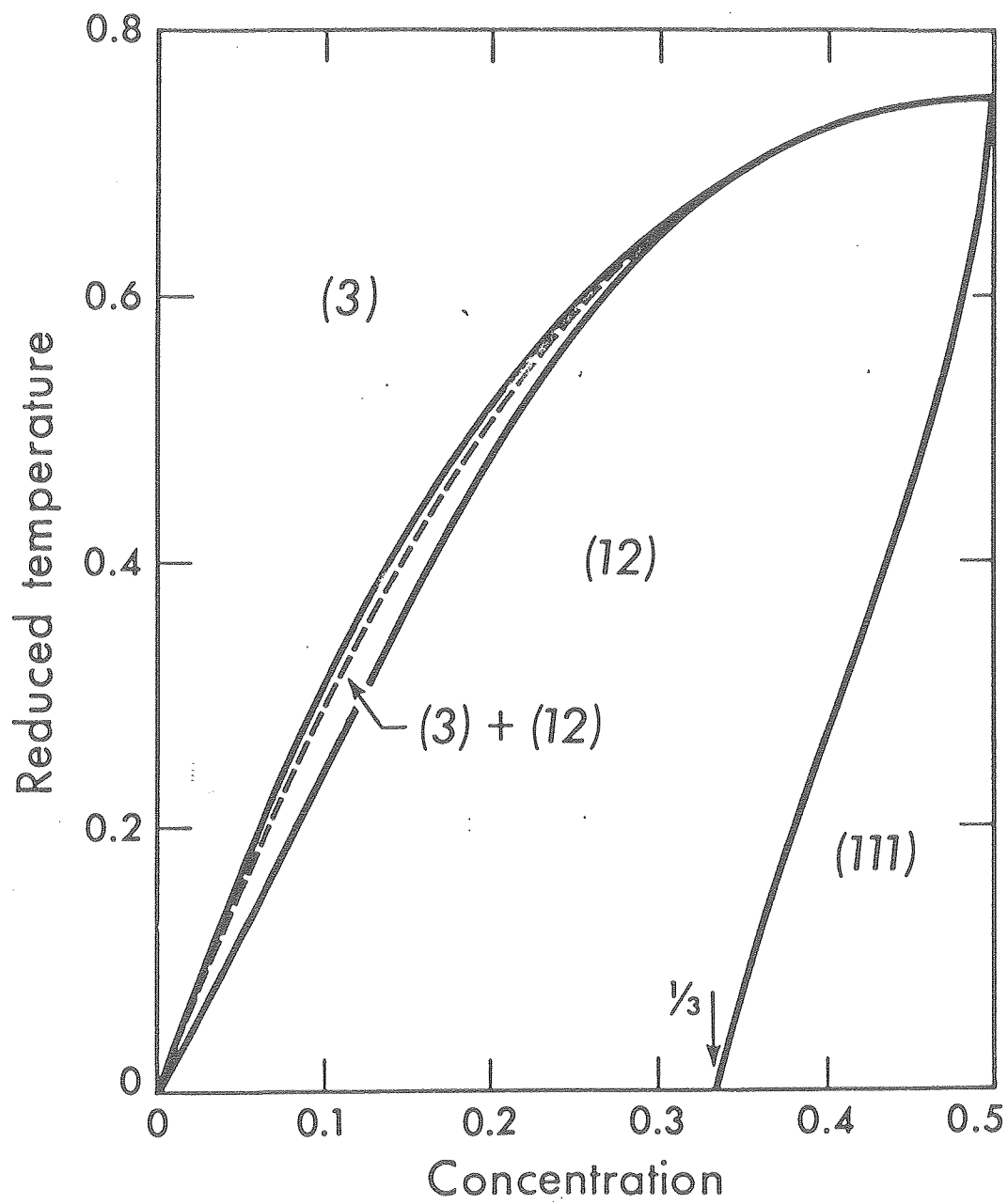


Figure 2

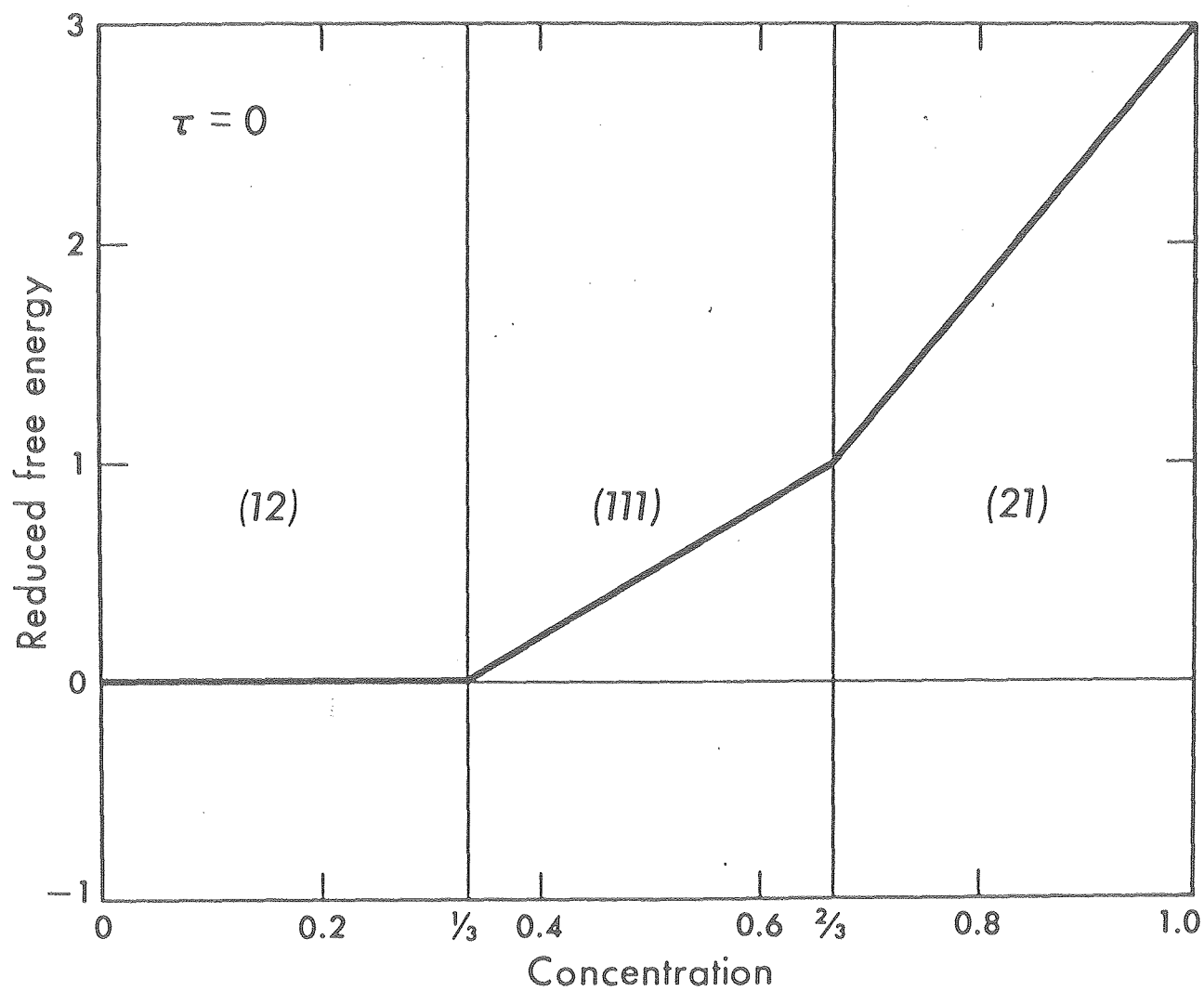


Figure 3

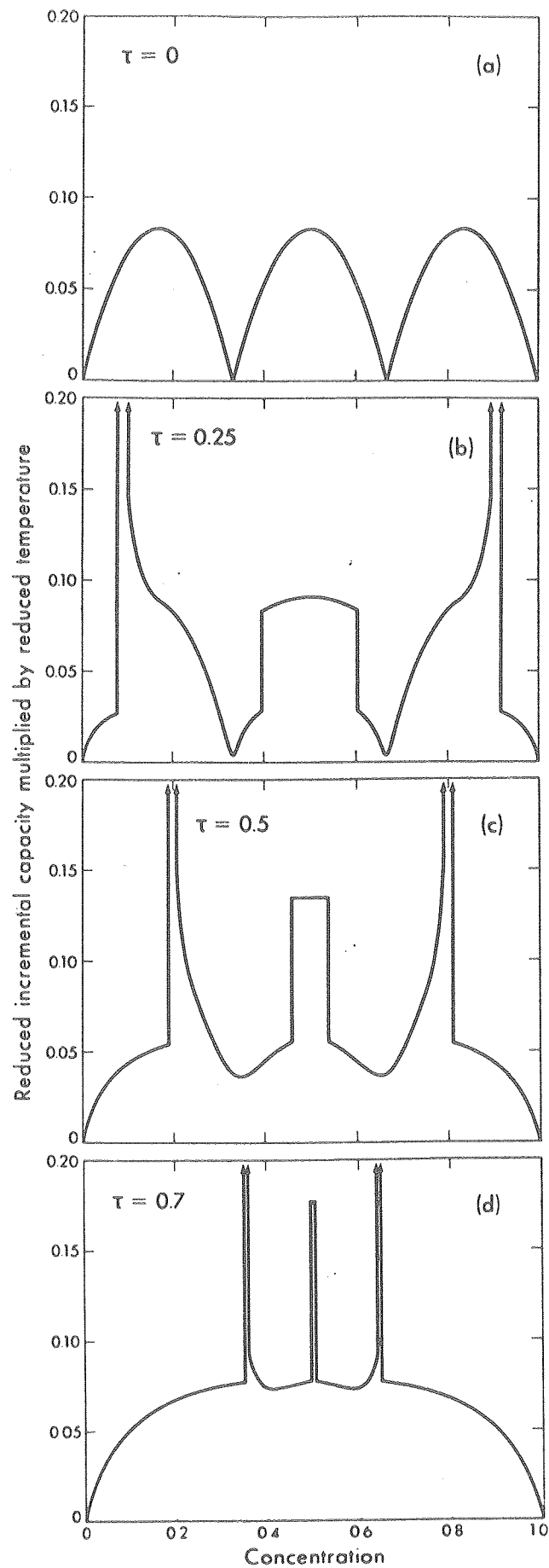


Figure 4

